Gate Control of Dynamic Nuclear Polarization in GaAs Quantum Wells

H. Sanada,[1] S. Matsuzaka,[1] K. Morita,[2,1] C. Y. Hu,[1,3] Y. Ohno,[1,3,*] and H. Ohno[1,2,†]

[1]*Laboratory for Nanoelectronics and Spintronics, Research Institute of Electrical Communication, Tohoku University, Katahira 2-1-1, Aoba-ku, Sendai 980-8577, Japan*

[2]*ERATO Semiconductor Spintronics Project, Japan Science and Technology Agency, Japan*

[3]*CREST, Japan Science and Technology Agency, Japan*

(Received 15 September 2004; published 8 March 2005)

Gate control of dynamic nuclear polarization under optical orientation is demonstrated in a Schottky-gated *n*-GaAs/AlGaAs (110) quantum well by time-resolved Kerr rotation measurements. Spin relaxation of electrons due to mechanisms other than the hyperfine interaction is effectively suppressed as the donor induced background electron density is reduced from metallic to insulating regimes. Subsequent accumulation of photoexcited electron spins dramatically enhances dynamic nuclear polarization at low magnetic field, allowing us to tune nuclear spin polarization by external gate voltages.

DOI: 10.1103/PhysRevLett.94.097601 PACS numbers: 76.70.Fz, 78.47.+p, 78.66.Fd, 78.67.De

Stimulated by experimental demonstration of NMR quantum computation in molecules [1], nuclear spins in semiconductors have attracted great interest because of their long coherence time as well as their compatibility of nanofabrication technologies for modern electronics [2]. In the proposed schemes, conduction electrons coupled via hyperfine interaction are employed to manipulate and detect the nuclear spin states with electrical and/or optical fields [3,4]. One of the advantages of semiconductor devices is the gate controllability of density and distribution of the electrons; it has been shown that the local nuclear polarization can be modulated through the change of the spin configuration in the quantum Hall regime [5] and displacement of the position of electron wave functions in a quantum well (QW) [6]. Here, we propose and demonstrate a gate control of nuclear spin polarization in a QW by a qualitatively different manner using the sensitivity of hyperfine interaction on the metal insulator (MI) phase transition. The dependence of hyperfine interaction on the doping density has been studied in bulk semiconductors [7–9]. In GaAs, isolated electron spins bound to donor impurity potential are strongly influenced by the random nuclear fields at low-doping level (insulating phase), whereas in metallic phase the D'yakonov-Perel' (DP) interaction, which is a spin-orbit interaction in crystals without inversion symmetry, becomes dominant for spin scattering and hyperfine interaction is less important [9]. Such a phase-dependent hyperfine interaction is expected to be present in two-dimensional (2D) electron systems, and thus one may also expect to be able to tune the degree of nuclear polarization by phase control through modulating 2D electron density by an external gate voltage.

In this Letter, we present an optical investigation of nuclear spin polarization in a gated *n*-GaAs/AlGaAs (110) QW, which provides 2D electrons with longer spin lifetime because of the suppression of DP and electron-hole exchange interactions at low temperatures. We employed a time-resolved Kerr rotation (TRKR) technique, which is one of the powerful tools to measure electron spin dynamics [10] and also nuclear polarization [11] in semiconductors. Optically excited nonequilibrium electron spins polarize lattice nuclei via hyperfine interaction [dynamic nuclear polarization (DNP)], and the effective magnetic field produced by the established nuclear polarization can be measured by TRKR data throughout the electron Larmor precession. We observed that DNP is drastically enhanced when the background 2D electron density n is reduced from metallic to insulating regime. The results clearly indicate the modulation of hyperfine interaction with the lateral extent of the electron wave function.

The sample we studied is a 7.5 nm-thick *n*-GaAs/$Al_{0.3}Ga_{0.7}As$ single QW grown on a (110)-oriented semi-insulating GaAs substrate by molecular beam epitaxy. The QW is Si doped (nominal doping density of 7×10^{17} cm^{-3}), and a 6×10^{11} cm^{-2} (3×10^{11} cm^{-2}) Si δ-doping layer is buried in the top (bottom)

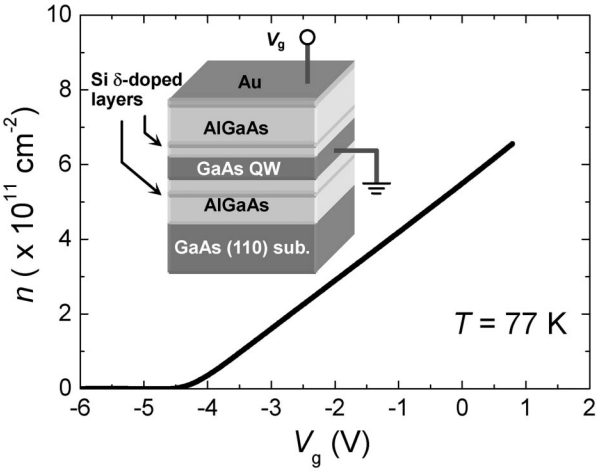

FIG. 1. The electron density n estimated by Hall and ac-capacitance measurements is plotted as a function of gate voltage V_g. Inset: cross-sectional view of the sample structure.

$Al_{0.3}Ga_{0.7}As$ barrier with a 20 nm (100 nm) spacer layer (see the inset of Fig. 1). A Hall-bar mesa with a 1 mm × 2 mm channel was made by a standard photolithograph technique and wet-chemical etching. Ohmic contacts to two-dimensional electron gas (2DEG) were formed by alloying AuGe/Ni, and a Schottky gate electrode was then made on the channel region by deposition of semitransparent Au film (~10 nm) and a lift-off technique. The gate voltage V_g is applied between the top gate and the Ohmic contacts (2DEG). Figure 1 shows V_g dependence of n examined at 77 K after irradiation of light by a Hall and ac-capacitance measurements. At $-4.0\ \mathrm{V} < V_g < 0.5\ \mathrm{V}$, the data can be fitted with a liner function $n = 1.30 \times 10^{11} \times (V_g - 4.23\ \mathrm{V})\ (\mathrm{cm}^{-2})$. The 2DEG is completely depleted at $V_g \sim -5$ V. These characteristics are virtually independent on the temperature below 77 K.

For the observation of temporal 2DEG spin dynamics and the detection of DNP, we employed a TRKR technique. We used a mode-locked Ti:sapphire laser with pulse duration of 100 fs and repetition rate of 76 MHz. The pulse train derived from the laser was divided into pump pulses (circular polarization) and probe pulses (linear polarization), and their relative delay time Δt was varied using a mechanical delay line. The Kerr rotation angle θ_K of the probe pulses was measured by using a balanced detector.

We first investigate the results of the V_g-dependent DNP. Figure 2(a) illustrates the experimental geometry. The sample was placed in an optical cryostat with a superconducting magnet so that the $[1\bar{1}0]$ axis in the QW plane is perpendicular to the external magnetic field $\boldsymbol{B}_{\mathrm{ext}}$, and the [001] axis was tilted by angle $\alpha = 45°$ with respect to $\boldsymbol{B}_{\mathrm{ext}}$. The incident angle of the pump and probe beams were also 45° with respect to the QW plane. At $\Delta t = 0$, a circularly polarized pump pulse excites spin polarized electrons in the QW. Subsequently, the electron spin $\boldsymbol{S}$ starts to precess about the vector $\boldsymbol{\Omega}_{\mathrm{tot}} = (\mu_B/\hbar)\hat{g}\boldsymbol{B}_{\mathrm{ext}} + (A/\hbar)\langle \boldsymbol{I} \rangle$ at the angular frequency $|\boldsymbol{\Omega}_{\mathrm{tot}}|$, where μ_B is Bohr magneton, $\hbar$ is the reduced Plank constant, $\hat{g}$ is an anisotropic g tensor in the QW, A is the hyperfine constant, and $\langle \boldsymbol{I} \rangle$ is the average nuclear spin [8]. When there exists a component parallel to $\boldsymbol{\Omega}_{\mathrm{tot}}$, the projection of the time evolution of $\boldsymbol{S}$ onto the QW normal is expressed as $S_\perp(t) = C_1 \exp(-\Delta t/T_1) + C_2 \exp(-\Delta t/T_2^*) \cos(|\boldsymbol{\Omega}_{\mathrm{tot}}|\Delta t)$, where C_1 and C_2 are constants, T_1 is the spin relaxation time, and T_2^* is the effective spin coherence time. The magnitude of $\theta_K(\Delta t)$ is assumed to be proportional to the magnetization induced by $S_\perp(\Delta t)$. Figure 2(b) shows $\theta_K(\Delta t)$ for several gate voltages in the range $-4.0\ \mathrm{V} < V_g < 1.4\ \mathrm{V}$ measured at 4.5 K. Here, the intensity of the pump beam I_{ex} was fixed at 5 mW, corresponding to the excitation of $2 \times 10^{10}\ \mathrm{cm}^{-2}$ spin polarized electrons per each pulse, while the probe beam intensity was fixed at 0.5 mW, which is believed to be low enough not to affect the observed TRKR signal and DNP. The applied $B_{\mathrm{ext}}(= |\boldsymbol{B}_{\mathrm{ext}}|)$ was set at 5 mT. At each V_g, the excitation photon energy E_{ex} was tuned so that the TRKR signal takes maximum value. The data in Fig. 2(b) reveal that when $V_g < 0$ V oscillations due to Larmor precession become observable and clearly resolved for $V_g < -1.5$ V. In Fig. 2(c), we plotted the oscillation frequency $|\boldsymbol{\Omega}_{\mathrm{tot}}|/2\pi$ from the data in Fig. 2(b) as a function of V_g. With decreasing V_g from 0 to −1.5 V, $|\boldsymbol{\Omega}_{\mathrm{tot}}|$ gradually increases and then saturates at ~0.7 GHz.

The appearance of the oscillation with decreasing V_g in Figs. 2(b) and 2(c) can be attributed to the enhanced DNP from the following observation. A characteristic feature of DNP was revealed in the I_{ex} dependence of $|\boldsymbol{\Omega}_{\mathrm{tot}}|$. Figure 3 shows $|\boldsymbol{\Omega}_{\mathrm{tot}}|$ with V_g fixed at −0.5, −1.0, and −2.0 V as a function of I_{ex}. $|\boldsymbol{\Omega}_{\mathrm{tot}}|$ increases with increasing I_{ex}, and tends to saturate at higher I_{ex} [8]. No oscillation was observed at $V_g = 0$ V and $B_{\mathrm{ext}} = 5$ mT. One should take into account that, by changing V_g, the n-dependent screening or band-filling effects can change the absorption coef-

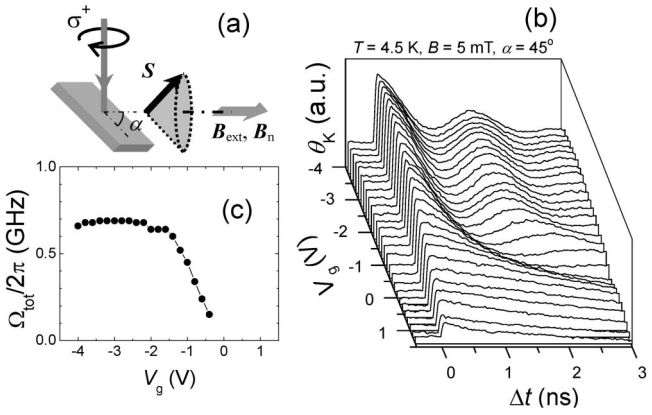

FIG. 2. (a) Geometry of the magneto-optical measurements. (b) Traces of the temporal Kerr rotation θ_K at $-4.0 \le V_g \le 1.4$ (V), $B_{\mathrm{ext}} = 5$ mT, and $T = 4.5$ K. (c) Larmor precession frequency $|\boldsymbol{\Omega}_{\mathrm{tot}}|/2\pi$ is plotted as a function of V_g.

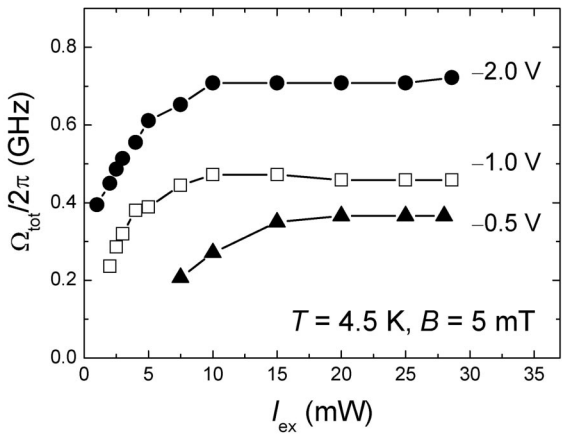

FIG. 3. Excitation intensity I_{ex} dependence of the Larmor precession frequency $|\boldsymbol{\Omega}_{\mathrm{tot}}|/2\pi$ is plotted for $V_g = -2$, −1, and −0.5 V.

ficient and thus the number of photoexcited electrons in the QW. These effects are, however, not significant in the present case since the maximum $|\mathbf{\Omega}_{\rm tot}|$ after saturation clearly depends on $V_{\rm g}$.

The contribution of the Zeeman term $|\hat{g}|\mu_{\rm B}B_{\rm ext}/\hbar$ to $|\mathbf{\Omega}_{\rm tot}|$ is also negligibly small for any $V_{\rm g}$ compared to the observed nuclear field at $B_{\rm ext} = 5$ mT. To confirm this, the $V_{\rm g}$ dependence of the g factor was examined by measuring Larmor precession in a different geometry where DNP is effectively suppressed [12]: the measurement was done at $B_{\rm ext} = 2$ T and 70 K with the QW plane slightly tilted ($\alpha = 4°$) with respect to $\boldsymbol{B}_{\rm ext}$. We found that the g factor at $\alpha = 4°$, i.e., $\sim g_{[001]}$, changes almost linearly with $V_{\rm g}$: $g_{[001]} = -0.03$, -0.04, and -0.05 for $V_{\rm g} = 0$, -1, and -2 V, respectively. The calculated $|\hat{g}(\alpha = 45°)| \sim 0.1$ at $V_{\rm g} = -1.5$ V corresponds to ~ 2 MHz at 5 mT, about 2 orders of magnitude smaller than the observed $|\mathbf{\Omega}_{\rm tot}|$ shown in Fig. 2(c).

Now we focus on the mechanism responsible for the enhanced DNP by applying negative $V_{\rm g}$. The degree of DNP should be determined by the contact hyperfine interaction $A\boldsymbol{I}\cdot\langle\boldsymbol{S}\rangle$, where $\langle\boldsymbol{S}\rangle$ is time-averaged electron spin. First we look into $\langle\boldsymbol{S}\rangle$, which corresponds to the nonprecessing component of $\boldsymbol{S}$ parallel to $|\mathbf{\Omega}_{\rm tot}|$ and depends on the time constant T_1. In the case of n-GaAs/AlGaAs (110) QW, T_1 becomes comparable or even longer than the pulse repetition time ($\Delta T \sim 13$ ns) at low temperatures [13]. This leads to the accumulation of photoexcited spins into the background 2DEG, reflected in the offset onto $\theta_{\rm K}$ just before pumping at $\Delta t = 0$. In fact, we found the $\theta_{\rm K}(\Delta t = -20$ ps) [equivalent with $\theta_{\rm K}(+13140$ ps)] varying with $V_{\rm g}$ as shown in Fig. 2(b): here we employed $\theta_{\rm K}(-20$ ps) as a measure of T_1 instead of acquiring it by fitting of $\theta_{\rm K}(\Delta t)$ at $B_{\rm ext} = 0$ T because of less accuracy for the limited time span of our delay-line system. In Fig. 4(a) $\theta_{\rm K}(-20$ ps) at $B_{\rm ext} = 0$ T is shown by a gray-scale plot as a function of $E_{\rm ex}$ and $V_{\rm g}$. The shape of Kerr rotation spectra [Fig. 4(b)] reflects the different population of spin-up and -down states [14]. As shown in Fig. 4(a), the center of the spectra is found redshifted with decreasing n, which is explained by the decrease of the Fermi energy and the Stark effect. In Fig. 4(c), we plot $\theta_{\rm K}(-20$ ps) at the same energies employed for measuring $\theta_{\rm K}(\Delta t)$ in Fig. 2(b), which are expressed by cross symbols in Fig. 4(a). A clear peak observed at $V_{\rm g} \sim -1.5$ V indicates that T_1 is not a monotonic function of $V_{\rm g}$ (and thus n) and spin is most preserved around $n = 3.5 \times 10^{11}$ cm^{-2}.

We proceed to quantitative discussion of the n dependence of DNP. In bulk n-GaAs, T_2^* has a peak (>100 ns) near the MI transition ($n_c \sim 10^{16}$ cm^{-3}) at low temperatures [9,15]. Above the critical density n_c, spin relaxation due to the DP mechanism is enhanced as the increased kinetic energy of electrons allows them to be delocalized and have longer momentum scattering time. Below n_c, the hyperfine interaction becomes predominant for isolated, localized electrons [9]. In a modulation-doped GaAs/AlGaAs (100) QW, T_1 and relevant spin relaxation mechanisms have been studied as a function of gate-controlled electron density [16]. Similar to the case of bulk n-GaAs, the DP mechanism governs T_1 at higher n (in metallic phase): spin preservation is most favored at the critical density $n_c \sim 5 \times 10^{10}$ cm^{-2}, at which the MI transition occurs. Below n_c, on the other hand, electron-hole exchange interaction is considered to be enhanced as a result of localization and weakened screening effect [16]. Note that in (100) QW, T_1 is of the order of a few hundred picoseconds in the whole range of $n < 1.4 \times 10^{11}$ cm^{-2}.

In the present case, the situation is different. First, the DP mechanism, which is a source of strong spin relaxation for 2DEG in (100) QWs, is effectively suppressed in (110) QWs even for higher n: only the residual higher order correction contributes to T_1 [17]. Second, MI transition occurs in doped QWs at relatively high doping density $\sim 10^{12}$ cm^{-2} [18]. In the present sample, the intensity of the photoluminescence due to the recombination of the electron-heavy hole pairs in the QW, measured at 9 K, indicates a rapid increase at $V_{\rm g} \sim -0.5$ V with decrease of $V_{\rm g}$. This is a sign of the electronic states being localized up to $n \sim 5 \times 10^{11}$ cm^{-2} (at $V_{\rm g} = -0.5$ V), whereas the screening effect of the excess free electrons suppressed the formation of exciton when $V_{\rm g} > -0.5$ V. In addition, the fact that the conductance of the 2DEG is also dropped across $V_{\rm g} \sim -0.5$ V strongly supports that the MI transition takes place at around $n \sim 5 \times 10^{11}$ cm^{-2} as observed in Refs. [16,19]. Correlation between the observation of the DNP and the MI transition across $n \sim 5 \times 10^{11}$ cm^{-2} suggests that the hyperfine interaction is more enhanced

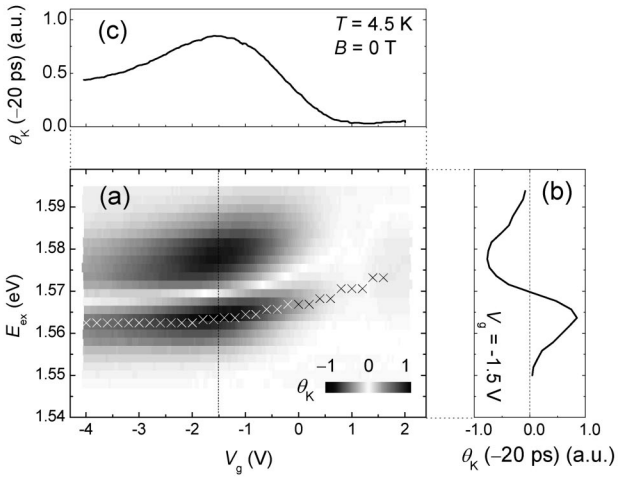

FIG. 4. Gate voltage $V_{\rm g}$ and excitation photon energy $E_{\rm ex}$ dependence of Kerr rotation $\theta_{\rm K}$ at $\Delta t = -20$ ps, 4.5 K, and $B_{\rm ext} = 0$ T. (a) Gray-scale mapping of $\theta_{\rm K}(\Delta t = -20$ ps) in a $V_{\rm g} - E_{\rm ex}$ space. (b) Kerr rotation spectra at $V_{\rm g} = -1.5$ V. (c) Peak $\theta_{\rm K}$ [indicated by cross symbols in (b)] is plotted as a function of $V_{\rm g}$.

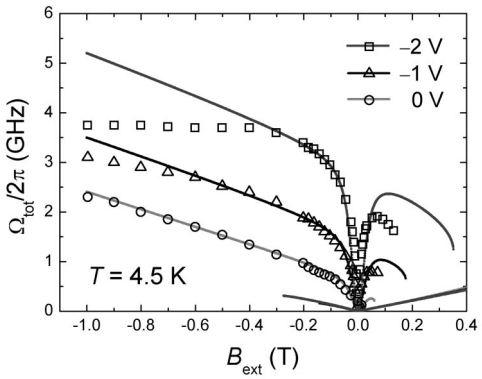

FIG. 5. External magnetic field B_{ext} dependence of Larmor precession frequency $|\mathbf{\Omega}_{tot}|/2\pi$ at 4.5 K and 5 mT for several V_g. Solid lines are the fitted results of the self-consistent calculation.

because of the occupation of localized states of electrons by reducing n with negative V_g. As $V_g > -0.5$ V, on the other hand, other spin relaxation mechanisms (probably higher order correction of DP or Elliot-Yafet mechanism [20]) should become dominant for itinerant electrons, resulting in less effective DNP.

Finally, we note that the effect of nuclear depolarization due to the effective local fluctuating field B_{loc} on the observed gate-controlled DNP is negligibly small. Recently B_{loc} of several tens of mT have been reported [13,21,22], which is much larger than the predicted dipole-dipole interaction between nuclei ($\sim$0.1 mT) [23]. We examined in the present sample the n dependence of the effective B_{loc} from the B_{ext} dependence of $|\mathbf{\Omega}_{tot}|$. In Fig. 5, we plot $|\mathbf{\Omega}_{tot}|/2\pi$ at $V_g = 0$, -1, and -2 V, which were obtained in the geometry of Fig. 2(a) as described above. The solid lines in Fig. 5 are the results of self-consistent calculation of coupled electron-nuclear spins with B_{loc} as a fitting parameter [13]. In the calculation, the anisotropic g tensor was set as $g_{[001]}(g_{[110]}) = -0.03(-0.18)$, $-0.04(-0.19)$, and $-0.05(-0.20)$ for $V_g = 0$, -1, and -2 V, respectively [13]. Except for $B_{ext} < -0.6(-0.3)$ T at $V_g = -1(-2)$ V, the calculation reproduced the experimental data quite well [24]: at any V_g, the drop of $|\mathbf{\Omega}_{tot}|$ near $B_{ext} = 0$ T can be fit by setting $B_{loc} = 30$ mT, indicating little effect of $V_g(n)$ on B_{loc}. The other parameter Afc, where f is a leakage factor and c is a ratio of $|\langle \boldsymbol{S} \rangle|$ to the initial electron spin component along $|\mathbf{\Omega}_{tot}|$, depends on V_g: at $V_g = -2$ V, the value is found to be about five times larger than that for $V_g = 0$ V.

In conclusion, a novel approach to control nuclear spin polarization under optical orientation is demonstrated in a Schottky-gated n-doped (110) QW. The origin of gatable enhancement of DNP in our system is attributed to density-dependent electron localization, which is supposed from V_g dependence of the electron spin accumulation. The demonstrated gate-controlled DNP in a n-doped semiconductor might be of assistance for efficient initialization or manipulation of quantum bits in the semiconductor based nuclear spin quantum computers.

The authors acknowledge F. Matsukura, K. Ohtani, T. Kita, and M. Kohda for useful discussions. This work was partly supported by Ministry of Education, Culture, Sports, Science, and Technology (MEXT), Japan Society for the Promotion of Science (JSPS), and the 21st Century COE program "System Construction of Global Network Oriented Information Electronics" at Tohoku University.

*Electronic address: oono@riec.tohoku.ac.jp
†Electronic address: ohno@riec.tohoku.ac.jp

[1] See, for example, L. M. K. Vandersypen *et al.*, Nature (London) **414**, 883 (2001); J. A. Jones, Fortschr. Phys. **48**, 909 (2000), and references therein.
[2] *Semiconductor Spintronics and Quantum Computation*, edited by D. D. Awschalom, N. Samarth, and D. Loss (Springer-Verlag, Berlin, 2002).
[3] B. E. Kane, Nature (London) **393**, 133 (1998).
[4] T. D. Ladd *et al.*, Phys. Rev. Lett. **89**, 17901 (2002).
[5] J. H. Smet *et al.*, Nature (London) **415**, 281 (2002); W. Desrat *et al.*, Phys. Rev. Lett. **88**, 256807 (2002).
[6] M. Poggio *et al.*, Phys. Rev. Lett. **91**, 207602 (2004).
[7] See, for example, U. Fasol and E. Dormann, Phys. Rev. B **66**, 075207 (2002), and references therein.
[8] *Optical Orientation*, edited by F. Meier and B. P. Zakarchenya (Elsevier, New York, 1984).
[9] R. I. Dzhioev *et al.*, Phys. Rev. B **66**, 245204 (2002).
[10] J. M. Kikkawa *et al.*, Science **277**, 1284 (1997).
[11] J. Stephens *et al.*, Phys. Rev. B **68**, 041307(R) (2003).
[12] G. Salis *et al.*, Phys. Rev. Lett. **86**, 2677 (2001).
[13] H. Sanada *et al.*, Phys. Rev. B **68**, 241303(R) (2003).
[14] A. V. Kimel *et al.*, Phys. Rev. B **62**, R10610 (2000).
[15] J. M. Kikkawa and D. D. Awschalom, Phys. Rev. Lett. **80**, 4313 (1998).
[16] J. S. Sandhu, A. P. Heberle, J. J. Baumberg, and J. R. A. Cleaver, Phys. Rev. Lett. **86**, 2150 (2001).
[17] M. I. D'yakonov and V. Yu. Kachorovskii, Sov. Phys. Semicond. **20**, 110 (1986).
[18] C. I. Harris, B. Monemar, H. Kalt, and K. Köhler, Phys. Rev. B **48**, 4687 (1993).
[19] G. Finkelstein, H. Shtrikman, and I. Bar-Joseph, Phys. Rev. Lett. **74**, 976 (1995).
[20] R. J. Elliot, Phys. Rev. **96**, 266 (1954).
[21] R. K. Kawakami and D. D. Awschalom, Science **294**, 131 (2001).
[22] D. Gammon *et al.*, Phys. Rev. Lett. **86**, 5176 (2001).
[23] D. Paget *et al.*, and , Phys. Rev. B **15**, 5780 (1977).
[24] Saturation and subsequent decrease of the nuclear field for large B_{ext} have been found and are discussed in Ref. [12] and references therein.